

# Chapter 1

## General Introduction

### 1.1 Overview and Organization

This dissertation focuses on the feasibility of using processing and migration techniques to enhance the seismic images of two types of faults that are difficult to map with conventional reflection studies: normal and blind thrust. It is organized in two main parts:

#### **Enhanced imaging of a normal fault with seismic reflection data**

Interest in fault reflections spans several decades (e.g., Swartz and Lindsey, 1942; Deacon, 1943; Robinson, 1945; Bortfeld and Hurtgen, 1960; Allenby, 1962; Young et al., 1990; Hole et al., 1996). They are of fundamental value for the correct positioning in space of faults and optimum stacking of depth migrated shot gathers. There have been very few attempts, however, to image directly steeply-dipping faults in deep crustal data (Louie et al., 1988; Louie and Qin, 1991; Pullammanappallil and Louie, 1993). This is mostly due to strong lateral velocity variations and the lack of reliable velocity models.

Most of academic research using seismic reflection data to investigate extensional tectonics is based on time imaging, in that lateral velocity variations are not considered. This is due to the fact that depth imaging requires reliable velocity models to migrate “reflected refractions” (e.g., Robinson, 1945; Allenby, 1962) and “straddle reflections” (e.g., de Bazelaire and Viallix, 1994) from steep fault planes into their true position. Motivation for this study comes from the need to image directly fault geometries that cannot be constrained using conventional time sections, and to help resolve the ongoing controversy of how crustal extension is accommodated at depth. Standard time imaging techniques provide a good starting point for subsequent depth imaging processing. Defining fault plane geometries demands, however, a reliable velocity model and detailed prestack imaging, including nonhyperbolic fault reflections exhibiting reverse (negative) moveout on record sections.

In Chapter 2, I present subsurface basin geometry and the geometry of a normal fault at shallow depth in Death Valley, California, through depth imaging, considering vertical and lateral velocity variations, of seismic reflection data. The aim of depth imaging is to depict better the shallow basin structure and to evaluate the uncertainty on the geometry and the location of the normal fault previously inferred on conventional time sections. I show how this is possible with the help of a reliable velocity model and prestack Kirchhoff depth migration. The velocity model is a refined version of the model presented by Pullammanappallil and Louie (1994a) and was kindly provided by Satish K. Pullammanappallil.

## Enhanced imaging of crustal faults with earthquake data

Improvements in hardware performance, software, and relatively inexpensive mass storage devices have made handling and interpreting large amounts of earthquake seismology data feasible (e.g., Benz et al., 1994). In fact, data multiplicity and availability has produced great interest in processing such information with techniques previously used in exploration seismology. There is increasing and renewed interest in acoustic processing and imaging of earthquake sources. Stacking (e.g., Shearer, 1994), common midpoint stacking (e.g., Chávez-Pérez and Louie, 1995; De Luca et al., 1997), slant stacking (e.g., Benz et al., 1994), imaging, migration, and backprojection (Rietbrock and Scherbaum, 1994; Ryzhikov et al., 1996; O'Doherty et al., 1997), etc, are now common terms and processes utilized in recent papers dealing with processing of earthquake data.

In Chapter 3, I present, along the lines of acoustic processing using earthquake sources, a new technique that images the reflectivity structure of crustal fault zones with simple data editing and prestack Kirchhoff depth migration of short-period earthquake recordings. The dominance of  $P$ -wave reflectivity over  $S$ -wave reflectivity from crustal fault zones suggests that variations in Lamé parameter  $\lambda$  (e.g., Telford et al., 1990, p. 143) control fault zone reflections. Reflections due to  $\lambda$  variations radiate isotropically, unlike the backscattering from impedance contrasts or the forward scattering from velocity contrasts. I then suggest that crustal faults may be distinguishable from non-tectonic crustal structures on the basis of this isotropic  $P$ -wave scattering. In Chapter 4, I show how this new crustal imaging

procedure uses short-period data in a cost-effective manner to depict crustal reflectivity images from the Los Angeles Basin that select for such isotropic reflectivity, preferentially showing crustal fault structure. My depth sections sum together backscattered and forward scattered arrivals from subsurface depth points, effectively filtering out simple impedance or velocity variations. In particular, imaging beneath the 1991 Sierra Madre aftershock zone shows the same lower crustal reflective zone below the San Gabriel Mountains that was imaged by the 1994 Los Angeles Region Seismic Experiment. This represents, to the best of my knowledge, the first step of high resolution imaging of complex three-dimensional structures with passive seismic data, using processing techniques commonly used for exploration seismology.

The two data sets I use do not exhibit clear raw data, and both were obtained in regions of complex geology. Because of this, we should expect limitations in the enhanced final images, as well as the need to do further work. In Chapter 5, I summarize the results of the previous chapters and make some suggestions for future research.

## **1.2 Method used in this study**

Throughout this work, I will refer to prestack Kirchhoff depth migration. The prestack Kirchhoff depth migration implementations I use are an extension of the previous work of Louie et al. (1988) and Louie and Qin (1991). John N. Louie is

the author of the bulk of the vital source code I utilize and describe in this work for doing migration, as well as of most of the basic data editing and manipulation routines.

Prestack Kirchhoff depth migration is not a new technique, but its practical implementation has been around for 20 years or so. Its origin goes back to the geometrical process described by Hagedoorn (1954) and it is the best established imaging technique in exploration seismology. It allows us to search for reflectors in the subsurface while handling an irregularly spaced distribution of sources and receivers. It has no dip limitations and its domain of application has been successfully tested and exploited in the oil industry for two- and three-dimensional targets, in both marine and land data.

Prestack Kirchhoff depth migration is essentially described by summation of seismograms along Huygens' surfaces assigned to each point of the imaging space. For doing this one assumes that scattering is due to small inhomogeneities (i.e., Born approximation; Aki and Richards, 1980, Vol. II, p. 731; Wu, 1989; Matson, 1996), that the media are acoustic, and consider only primary reflections, optical rays between scatterers, and far-field waves. In simple terms, Huygens' principle (whose publication predates Hagedoorn's 1954 paper by nearly 300 years) states that accurate images of reflected data can be produced by summation (integration). To provide an image at any given location, one needs only to sum the recorded data over an appropriate diffraction (scattering) surface. The main steps behind a two- (2-D) or three-dimensional (3-D) prestack Kirchhoff depth migration using

traveltime tables can be summarized as follows:

1. Calculate traveltimes for different sources and receivers.
2. Access traveltime tables to perform Kirchhoff summation of the input seismic data.

Fig. 1.1 shows how, for the 2-D case and a constant velocity medium, the locus of possible reflection points is an ellipse, or Kirchhoff trajectory, with the source (s) and receiver (r) as foci. The sketch includes three reflected rays that define the Kirchhoff trajectory. This ellipse represents the impulse response of the (2-D) prestack Kirchhoff depth migration operator (e.g., Claerbout, 1985, p. 26-29). Also for a constant velocity earth, the impulse response of full 3-D prestack migration is an elliptical bowl or ellipsoid. For a variable-velocity medium, these Kirchhoff trajectories become distorted. Fig. 1.2 shows the two-way traveltime imaging condition. This is very similar to the focusing of light by a lens, where the focal length is determined by the velocity field used to compute the traveltimes (Maeland, 1996).

Born inversion and imaging methods are the most widely used in exploration seismology (e.g., Weglein, 1985; Carrion, 1987; Matson, 1996). For instance, in seismic tomography, the scattered wavefield is backpropagated, using the scalar wave equation, after linearization through application of either the Born or Rytov approximation (e.g., Lo et al., 1988). Within these approximations, the solution of a partial differential equation is expressed as a perturbation about a known solution

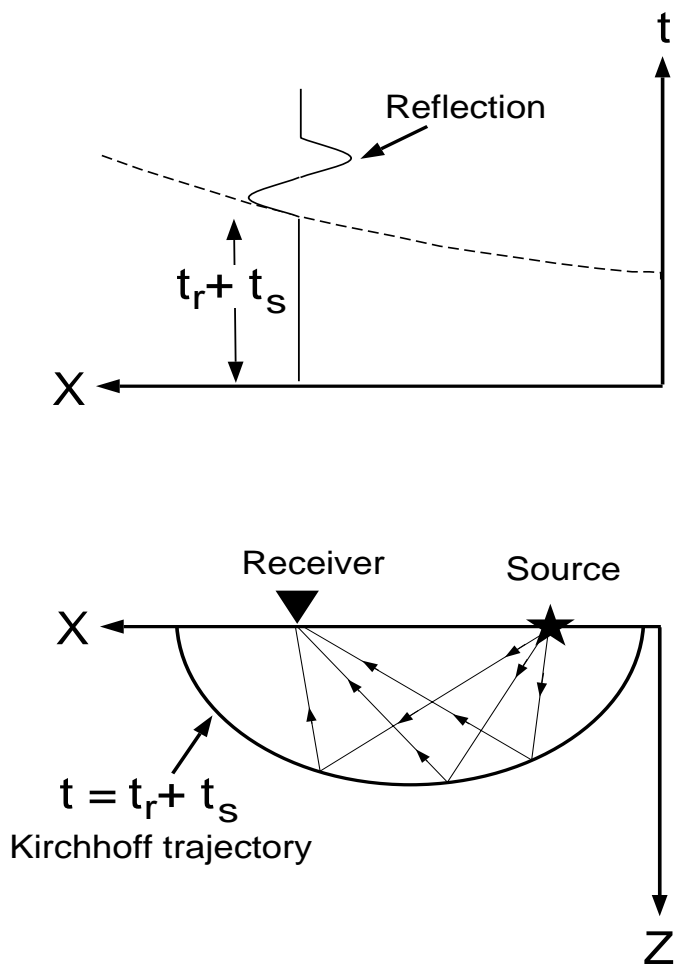


Figure 1.1: For a constant velocity medium, the locus of constant reflection time of all possible reflection points is an ellipse, or Kirchhoff trajectory (defined by traveltime  $t$ ), with source (s) and receiver (r) as foci.  $t_s$  and  $t_r$  stand for the traveltimes from the source and receiver to the reflection or scattering point, respectively.  $t = t_s + t_r$  defines the total, two-way traveltime imaging condition.  $X$  stands for offset or source-receiver distance and  $Z$  stands for depth.

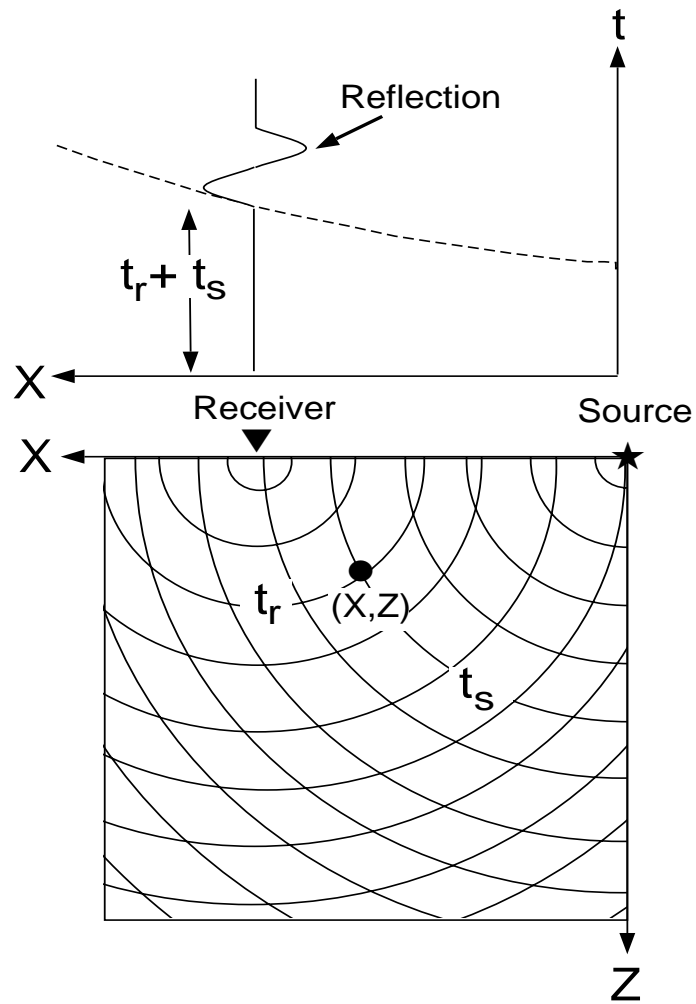


Figure 1.2: Contribution from a source-receiver pair to a depth point based on the two-way travelt ime imaging condition  $t = t_s + t_r$  (modified after Reshef and Kosloff, 1986). Curves in the X-Z plot depict isochrons or lines of equal time.

to a simpler equation (Matson, 1996). Thus, the inverse acoustic backscattering problem (i.e., determining medium geometries and/or properties from reflections) described, for instance, by diffraction tomography (Wu and Toksöz, 1987; Lo et al., 1988), is equivalent to the migration process.

Migration is a backprojection of primary reflection amplitudes into a depth section. It produces an image by constructive interference of all the source-receiver contributions. Data are considered to be linear superpositions of rays from individual point scatterers. The scattering potential of the medium can thus be estimated as the sum of the reflections recorded by each source-receiver pair, positioned according to the compressional,  $P$ -wave traveltimes of the rays between the surface points and the subsurface reflector. This is done using a two-way reflection traveltimes for the imaging condition. Fig. 1.3 shows how superposition of all contributions, despite smearing of energy along ellipses (also known as “smiles”), produces an image of the reflector in the  $X - Z$  space by constructive interference along the reflector, and destructive interference off it.

For the 3-D case of earthquake sources, the elliptical Kirchhoff trajectory becomes a bowl or ellipsoid with one buried focus (source). This turns out to be one of the most burdensome aspects of this imaging process because it obscures the resulting images. For the sake of illustration, Fig. 1.4 shows a sketch of the sequence I follow in this work to migrate earthquake record sections.

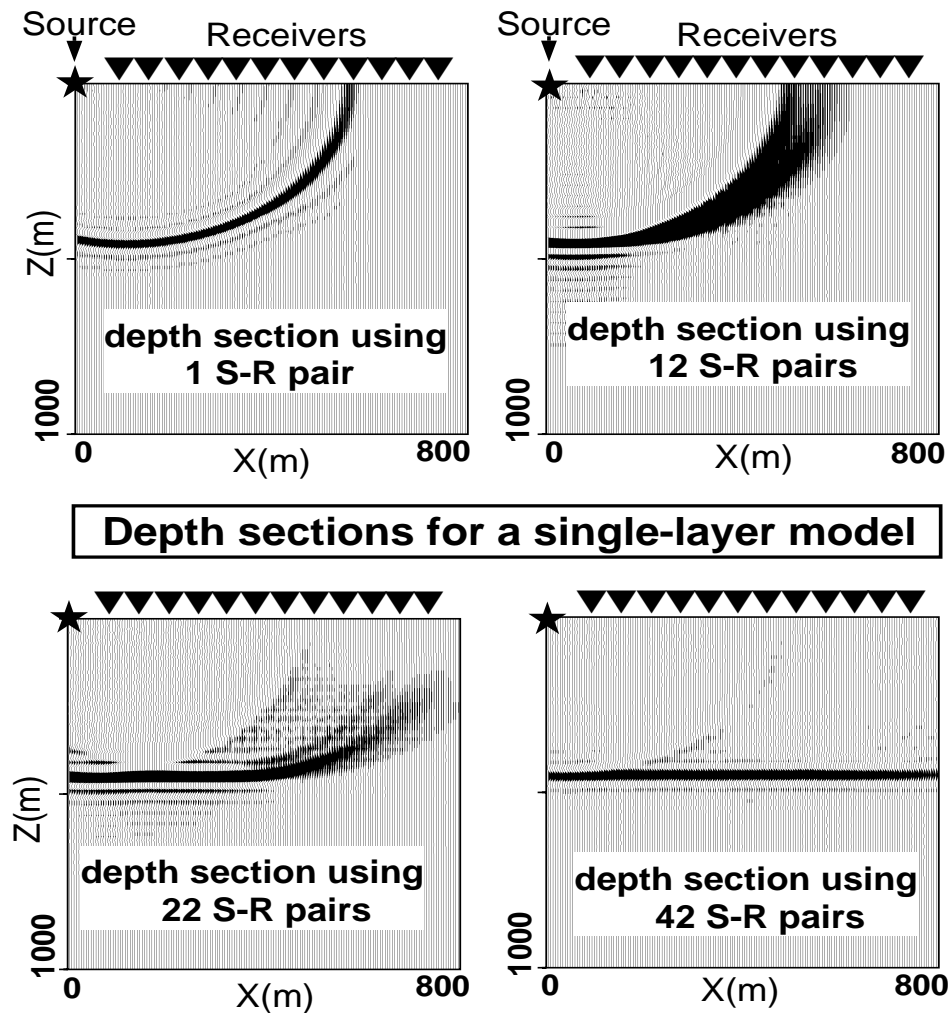


Figure 1.3: Depth sections for a single-layer model, showing contributions from one, twelve, twenty-two, and forty-two source-receiver (S-R) pairs. Superposition of all contributions produces an image of the reflector in  $X - Z$  space by constructive interference along the reflector and destructive interference off it. Note how the Kirchhoff trajectories cancel out as the number of contributions increases [modified after Hu and McMechan (1986) and Reshef and Kosloff (1986); courtesy of Satish K. Pullammanappallil].

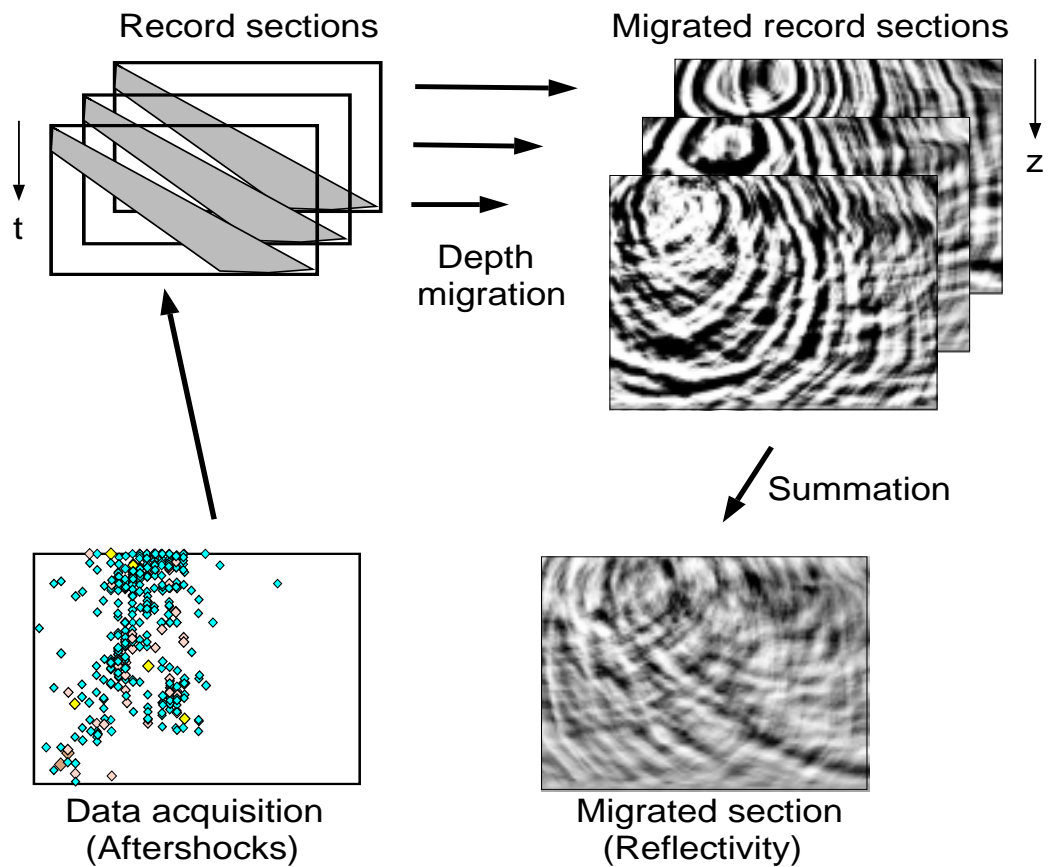


Figure 1.4: Schematic outline of migration of earthquake record sections. The depth migration process performs the mapping from time  $t$  into depth  $z$ . Each record is migrated individually along a migration profile. The final crustal reflectivity section arises from horizontal, pixel by pixel summation of each migrated record section. The gray fan in the record sections defines the part of the data used for migration. It includes the compressional,  $P$ -wave portion of the seismograms.

### 1.3 Fault zones

Scattering is the product of elastic heterogeneity. It is due to variations in shear ( $V_S$ ) and compressional ( $V_P$ ) wave velocities and density. Meter-scale and larger cracks and faults appear to play a dominant role in crustal scattering (Aki, 1995; Revenaugh, 1995c; Revenaugh and Reasoner, 1997). Exploration seismologists find that variations in  $P$ -velocity anisotropy dominate the reflectivity of exhumed mylonitic fault zones, producing stronger  $P$ -wave than  $S$ -wave reflectivities (Mooney and Ginzburg, 1986; Mooney and Meissner, 1992; McCaffree and Christensen, 1993). On the other hand, overall variations in density or rigidity dominate most other types of geologic contrasts, such as pluton boundaries; resulting in stronger  $S$ -wave reflectivities.

Experimental work shows wide ranges of  $V_P/V_S$  ratios within fault zones, on the basis of seismic velocity and density measurements made on samples from exhumed faults. For instance, McCaffree and Christensen (1993) showed, for the mylonite zone of the Brevard fault, that the compressional reflectivity will normally be stronger than the shear reflectivity. This stronger compressional reflectivity appears to be related to a wider distribution of compressional versus shear velocity values, creating stronger  $P$ -wave reflection coefficients and impedance variations.

However, earthquake seismologists at present have data sets that can be modeled by fault zones as only low-velocity layers. This is because of the recent, abundant work related to fault-zone trapped waves (e.g., Ben-Zion and Malin,

1991; Li et al., 1994a, b; Li and Vidale, 1996; Malin et al., 1996; Li et al., 1997). Because of this, I consider two models of fault zones in Chapter 3: one that produces strong compressional reflectivity (Mooney and Ginzburg, 1986; McCaffree and Christensen, 1993) and one with same material properties of the model Igel et al. (1997) used to simulate  $SH$ - and  $P - SV$ -wave propagation in fault zones.

See Appendices A and B for further details about fault and elastic properties, respectively.